

Phase Separation in Binary Fluid Mixture with Quenched Disorder

Rounak Bhattacharyya and Bhaskar Sen Gupta

Department of Physics, School of Advanced Sciences,

Vellore Institute of Technology, Vellore, Tamil Nadu - 632014, India

(Dated: March 19, 2022)

Abstract

Quenched or frozen-in, structural disorder is ubiquitous in real experimental systems. Much of the progress is achieved in understanding the phase separation of such systems using diffusion-driven coarsening in Ising model with quenched disorder. But there is a paucity of research in the phase-separation kinetics in fluids with quenched disorder. In this letter, we present results from a detailed Molecular dynamics (MD) simulation the effects of randomly placed localized impurities on the phase separating kinetics of binary fluid mixture. Our system resembles the fluid imbibed into a porous medium. We observe a dramatic slowing down in the pattern formation with increasing pin particle concentration. The domain growth follows the power-law with a disorder-dependent exponent. Due to the energetically favorable positions, the domain boundary roughens which modifies the correlation function and structure factor to a non-Percolation behavior. The correlation function and structure factor provide clear evidence that the superuniversality does not hold in our system.

Introduction.— Research attention in statistical physics has developed rapidly to understand the out of equilibrium phenomena over the past few decades. In this context, there is a paramount interest to investigate the evolution of a phase separating multi-component mixture with time, due to its application in diverse fields, e.g., magnetic materials, colloidal mixtures, polymer solutions, glasses, metallic alloys, binary liquids [1–5]. When a system of homogeneous multicomponent mixture is rendered thermodynamically unstable by a swift quench inside the miscibility gap, domains with different ordered phases form and expand with time until the system attains a local equilibrium. The domain coarsens due to the organization of matter, mostly dominated by diffusion and can be seen in almost all phase separating systems [6–18].

A *single time dependent characteristic length* $\ell(t)$ usually characterizes the domain growth pattern or domain morphology [5]. The same can be obtained by calculating two point equal time correlation function $C_{\psi\psi}(\vec{r}, t)$, where \vec{r} is the distance between two spatial points and t is the time after quench. So far, it is well demonstrated that pattern formation or coarsening of domains is a scaling phenomenon and exhibits the form $C_{\psi\psi}(\vec{r}, t) = g[r/\ell(t)]$ [19] where $g(x)$ is the scaling function. The average domain size $\ell(t)$ follows the power law: $\ell(t) \sim t^\alpha$, α defines the growth exponent. The value of the exponent depends on the apposite coarsening mechanism which drives phase separation.

Coarsening mechanism depends on the character of the system. For instance, in solid-solid mixtures (e.g., metallic alloys), diffusion dominates the domain growth whereas hydrodynamic effects contribute significantly in fluid-fluid mixtures. For the earlier the growth exponent $\alpha = 1/3$ which is attributed to Lifshitz-Slyozov (LS) law [5, 20]. This diffusive regime is very transient in fluid-fluid mixtures and we experience a prompt crossover from diffusive to the hydrodynamic regime. Here α takes two distinct values, viz., $\alpha = 1$ in viscous hydrodynamic regime followed by the inertial hydrodynamic regime with $\alpha = 2/3$. The above values of growth exponent are universal and pertinent to pure and isotropic systems [7, 8].

However, almost all real systems have local randomly frozen heterogeneities known as quenched disorder. It acts as a background random potential for the fluctuating degrees of freedom. The ever-present random disorder strongly influences the kinetics of phase separation and the domain morphology. Numerous studies have been performed so far to understand the diffusion-driven coarsening in Ising systems with quenched disorder [21–30]. But the phase-separation kinetics in fluids with quenched disorder is still in its infancy. In this letter, we undertake an extensive numerical study of domain growth dynamics of an immiscible symmetric binary fluid mixture in

the presence of quenched disorder. The disorder is introduced by randomly positioned pinning of particles in the system. Our system resembles phase separation of fluid in random porous materials [31–35] which are of great technological interest in the industry and oil recovery process.

Numerical simulations.— For our present analysis we perform a three-dimensional (3D) molecular dynamics (MD) simulation on a binary liquid in the NVT ensemble. We consider a 50 : 50 mixture of A and B particles at high density $\rho = N/V = 1$, where N and V represent the number of particles and volume of the system respectively. The two species interact via Lennard-Jones (LJ) potential

$$U_{\alpha\beta}(\vec{r}) = 4\epsilon_{\alpha\beta} \left[\left(\frac{\sigma_{\alpha\beta}}{\vec{r}} \right)^{12} - \left(\frac{\sigma_{\alpha\beta}}{\vec{r}} \right)^6 \right] \quad (1)$$

where $\vec{r} = |\vec{r}_i - \vec{r}_j|$ and $\alpha, \beta \in A, B$. To ensure energetically favorable phase separation, the parameters in the LJ potential are chosen as follows: $\sigma_{AA} = \sigma_{BB} = \sigma_{AB} = 1.0$ and $\epsilon_{AA} = \epsilon_{BB} = 1.0, \epsilon_{AB} = 0.5$. The choice of our interaction strength corresponds to the critical temperature $T_c = 1.42$, outlying the possible liquid-solid and gas-liquid transition point [36]. The temperature is measured in units of ϵ/k_B , where k_B is Boltzmann’s constant. Length is measured in units of σ . For simplicity we set the mass m_0 of all the particles and k_B equal to unity. For the sake of computational efficiency, the interaction potential is truncated to zero at $r_c = 2.5\sigma$. Periodic boundary condition is applied in all three directions.

To incorporate the effect of quenched disorder, we introduce randomly placed pinned (localized) particles in the system. These particles do not participate in the dynamics and stay frozen in their respective positions. The mobile particles interact with the pinned particles via the LJ potential. The density of the pinned particle is chosen such that $\rho_P \ll \rho_0$ where ρ_P and ρ_0 are the densities of the pinned and not pinned particles respectively with $\rho = \rho_P + \rho_0$. Our simulation is accomplished with five different pinning concentrations. We performed the MD simulation using the Velocity Verlet algorithm [37] over a total of 262144 ($= 64^3$) particles for each pinning percentage. We begin our simulation by preparing a well equilibrated homogeneous mixture at high temperature $T = 10.0$ followed by a quench to $T = 0.77T_c$ at $t = 0$. Here the reduced unit of time is taken as $\sigma\sqrt{m/\epsilon}$. Temperature is controlled by using the Nose-Hoover thermostat (NHT) which preserves the hydrodynamic effect [38]. Finally, the system is allowed to evolve to the thermodynamically favored state until the complete phase separation is achieved. The ensemble average of all the statistical quantities is obtained from 10 independent runs at $0.77T_c$ starting from completely different initial configurations.

To characterize the domain morphology and study the domain growth we introduce the two point

equal time correlation function $C_{\psi\psi}(\vec{r}, t)$ as follows:

$$C_{\psi\psi}(\vec{r}, t) = \langle \psi(0, t) \psi(\vec{r}, t) \rangle / \langle \psi(0, t) \rangle^2 \quad (2)$$

where the order parameter $\psi(\vec{r}, t)$ is obtained as follows: we compute the local density difference $\delta\rho = \rho_A - \rho_B$ between the two species A and B, calculated over a box of size $2\sigma^3$ located at \vec{r} . The $\psi(\vec{r}, t)$ is assigned a value $+1$ when $\delta\rho > 0$, and -1 otherwise. The angular brackets indicate the statistical averaging. We have also computed structure factor $S(\vec{k}, t)$ by taking the Fourier transform of the correlation function given by

$$S(\vec{k}, t) = \int d\vec{r} \exp(i\vec{k}\cdot\vec{r}) C_{\psi\psi}(\vec{r}, t) \quad (3)$$

to investigate the structural changes of the system. Finally for the isotropic system, spherically averaged $C_{\psi\psi}(r, t)$ and $S(k, t)$ are computed.

Numerical Results.— The effect of impurity on the phase separation dynamics is depicted in Fig. 1. Here we show the configurations obtained from our simulation for three different ρ_P at time $t = 2000$. It is observed that the kinetics of ordering slows down drastically with ρ_P . The pinned particles localize the domain walls in energetically favorable positions. However, this is overcome by the thermal energy due to sufficiently high temperature. It is worth noting in Fig. 1 that the domain boundary becomes rough with impurity. This is evident from the 2D cross-sectional plot of the configurations. The implication of the modified domain boundary will be discussed shortly in terms of the correlation function and structure factor.

In Fig. 2 we show the scaling plot for $C_{\psi\psi}(r, t)$ vs $r/\ell(t)$, where $\ell(t)$ is the average domain size. There are quiet a few ways to quantify the $\ell(t)$, e.g, first zero crossing of $C_{\psi\psi}(r, t)$, half-crossing of $C_{\psi\psi}(r, t)$, inverse of the first moment of $S(k, t)$. We have used the first method to calculate $\ell(t)$. An excellent data collapse is observed for different times when the same disorder concentration is considered. This suggests that even in the presence of disorder (fixed ρ_P), the system belongs to the same dynamical universality class [20]. However, the correlation function gets modified when the ρ_P changes and they do not overlap with each other when plotted at a fixed time t . This is shown in Fig. 2. For the pure system the $C_{\psi\psi}(r, t)$ shows a linear behavior at small r following the Porod law. However, in the presence of impurity, a nonlinear or cusp nature is observed, which can be attributed to the scattering from the rough domain boundary [39]. Therefore, the quench disorder results in breaking down the Porod law in the correlation function [40].

The evolution morphology is best realized in terms of the domain size ℓ . In Fig. 3 we show the

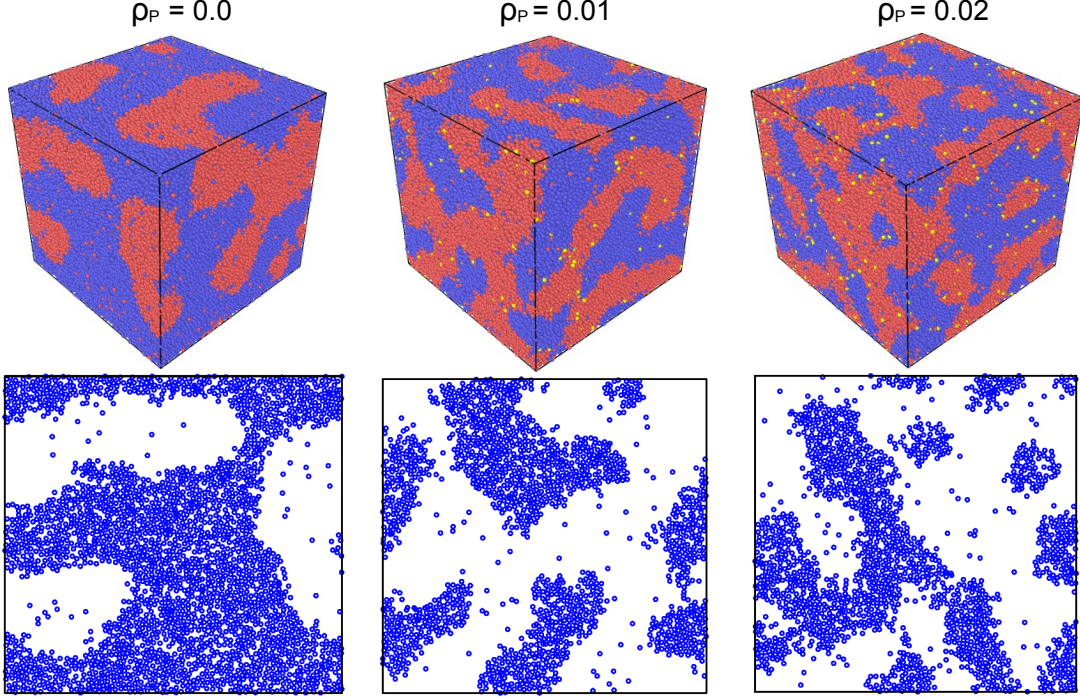


FIG. 1: Typical snapshots of our system for the impurity concentrations $\rho_P = 0.0, 1.0$ and 2.0 at time $t = 2000$ (LJ unit) are shown in the upper panel (left to right) at $T = 0.77T_c$. The A, B and pinned particles are marked as red, blue and yellow respectively. A two dimensional cross sectional area of the configurations in the upper panel with one type of particles A is shown in the lower panel.

time dependence of $\ell(t)$ for different impurity concentration. Our simulation is able to access the viscous hydrodynamic regime after an initial transient period. However, the growth rate slows down and the total time taken for the system to be completely phase-separated increases significantly with increasing impurity. This is consistent with the observation in Fig. 1.

To gain more insight into the disorder-dependent growth dynamics, we compute the instantaneous slope of $\ell(t)$ with time. This is best appraised by the instantaneous dynamical exponent $z_{\text{eff}} = 1/\alpha_{\text{eff}}$ where $\alpha_{\text{eff}} = d(\ln \ell(t))/d(\ln t)$. The result is shown in Fig. 4. In the absence of impurity, the exponent $\alpha_{\text{eff}} \sim 1$ in the viscous hydrodynamic regime. This is in accordance with our expectation [5]. In the presence of quenched disorder, the z_{eff} vs t curve exhibits a flat behavior for the intermediate and long time, indicating a power-law domain growth (\bar{z}) throughout the phase separation process. However, the exponent decreases gradually with ρ_P due to the slowing down of ordering. The variation of \bar{z} with ρ_P yields $\bar{z} \sim \rho_P^{0.25}$ as shown in Fig. 4.

In the presence of disorder, the relaxation mechanism changes from purely energy lowering to

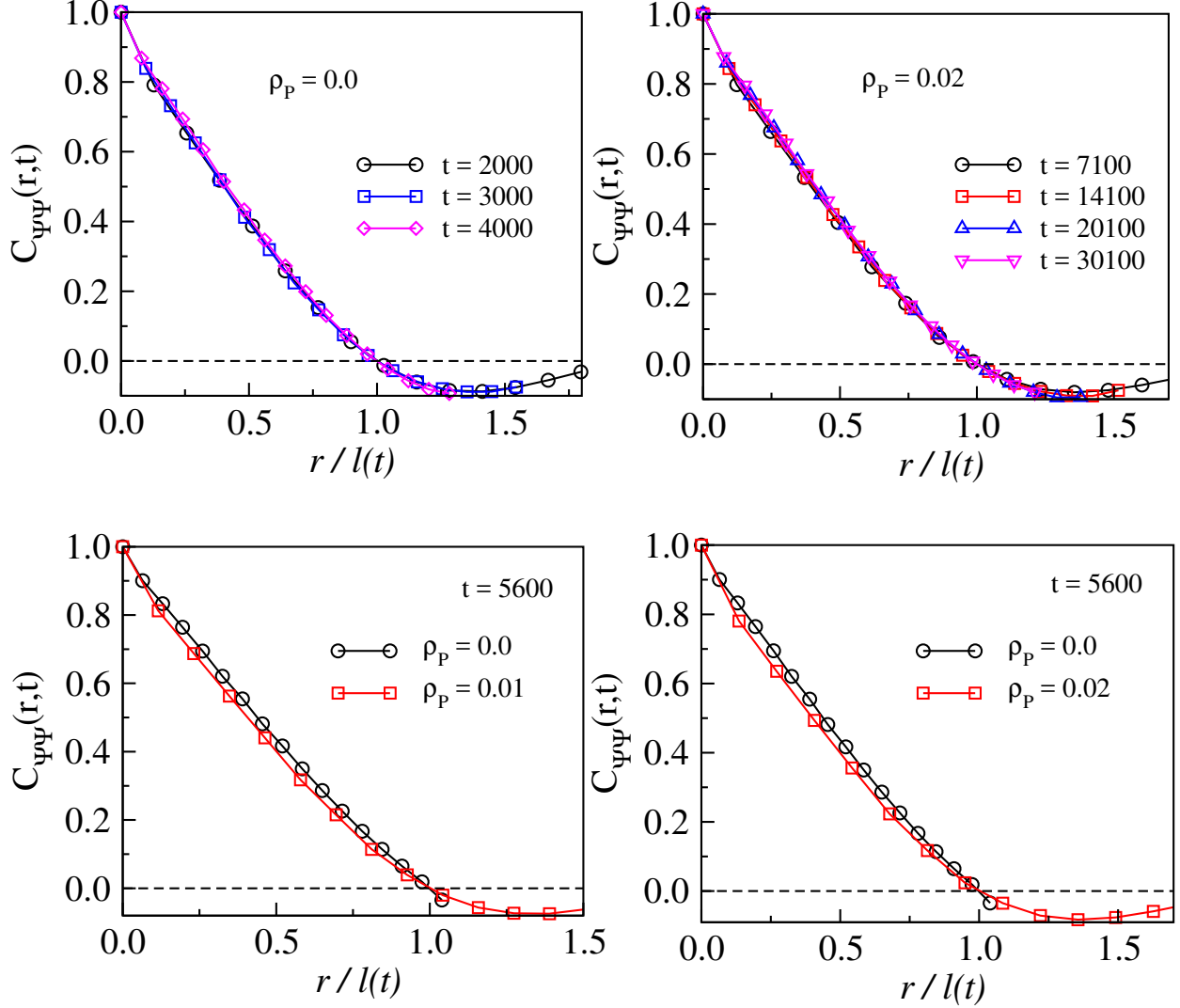


FIG. 2: Upper panel: the scaling plots for $C_{\psi\psi}(r,t)$ vs $r/l(t)$ are shown for the pure (left) and disordered system (right). Lower panel: we show the comparison for the same between the pure and disordered systems.

thermally activated process, due to the creation of energy barriers. The presence of the energy barrier slows down the relaxation process. An important issue in this regard is the so-called superuniversality (SU), i.e, whether the disorder-dependent spatial autocorrelation function scales to a master curve when the length is rescaled with respect to the domain size $\ell(t)$ [41, 42]. From Fig. 2 it is conspicuous that our system does not fall into the SU class. We also observe an algebraic domain growth throughout the phase separation process with a disorder-dependent exponent. This implies that the barrier size does not depend on the domain size for a given ρ_p .

In Fig. 5, we show the scaled structure factor $S(k,t)\ell^{-3}$ vs ℓk plot for different ρ_p in log-log

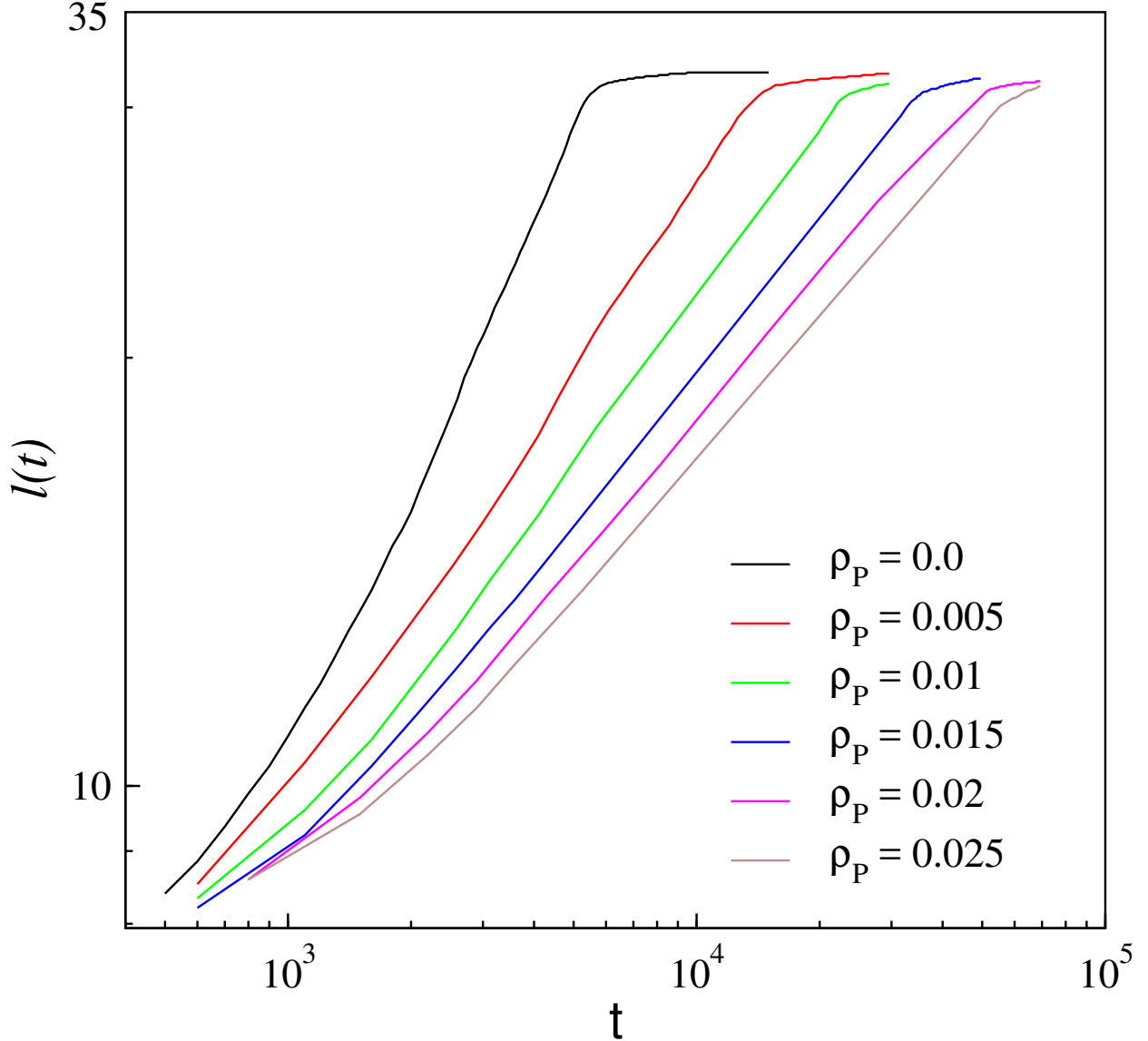


FIG. 3: The time evolution of the average domain size $\ell(t)$ is shown for different ρ_P in the log-log scale.

scale. Although, the decaying part of the tail for the pure system shows the Porod law behavior $S(k, t) \sim k^{-(d+1)}$ [20], the systems with immobile impurities shows a non-Porod behavior, $S(k, t) \sim k^{-(d+\theta)}$, where $\theta \simeq 0.5$. This value is very close to the results observed in the 3D random field ising model [39]. This substantiates the roughening of the domain interfaces with the increasing pinned particles and the violation of SU.

Summary and Discussion.—In summary, we have examined the kinetics of phase separation in a binary liquid in the presence of quench disorder. The disorder was obtained by pinning of particles at random positions in the system. We have observed that the dynamics of ordering slows down

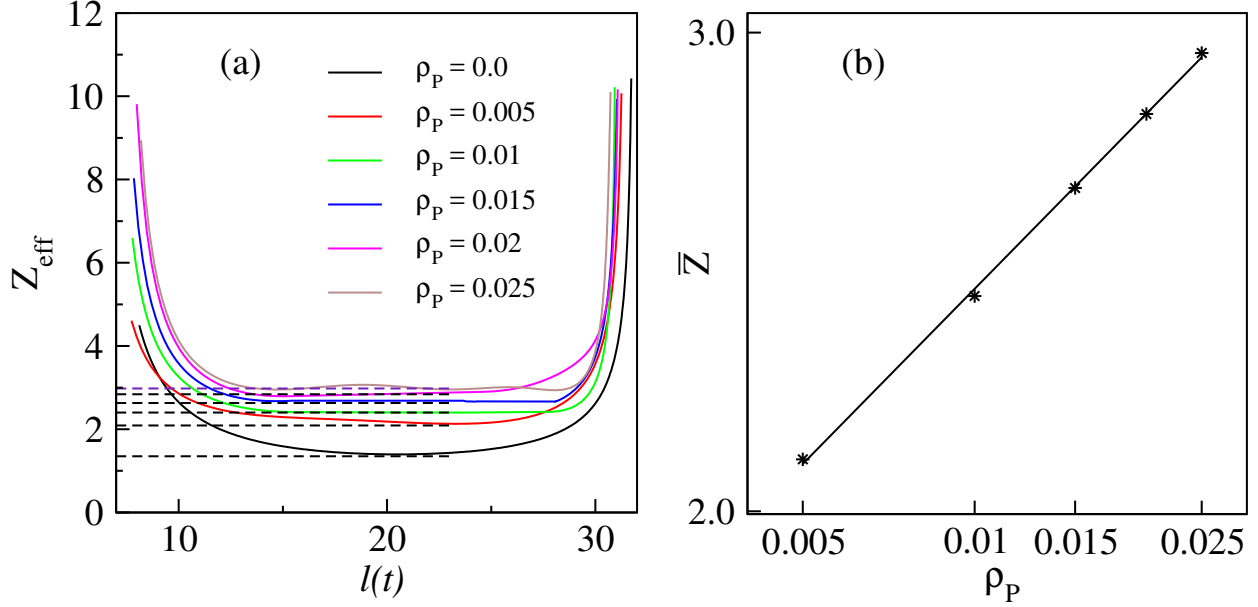


FIG. 4: (a) The instantaneous dynamical exponent z_{eff} vs the average domain size $l(t)$ is shown for different ρ_P . (b) z_{eff} vs t (points) plotted on a log-log scale. The solid line is the power law fitting with exponent 0.25 (see text).

dramatically with the concentration of localized particles. The spatial correlation function scaled with domain size shows disorder dependence and non-Porod behavior which can be attributed to the roughening of domain boundaries. The pure system clearly exhibits power-law domain growth with exponent unity in the viscous hydrodynamic regime. In the presence of disorder, the nature of growth still remains algebraic but the exponent decreases with impurity concentration. The disorder localizes the domain wall and creates energy barrier which is overcome by the thermally activation process. However, the algebraic domain growth conforms to the domain size-independent energy barrier throughout the phase separation process. We have also examined the structure factor for our system. The decaying part of the structure factor gets modified in the presence of disorder and shows non-Porod tail. Both the spatial correlation function and the structure factor do not obey superuniversality. We believe that our model and the results presented here offer a method to control the phase separation dynamics in real systems by adding quenched disorder appropriately. Studies following this line of thought will be presented elsewhere.

Acknowledgement.—The authors acknowledge useful discussions with J. Midya. B.S.G. acknowledges Science and Engineering Research Board (SERB), Dept. of Science and Technology (DST),

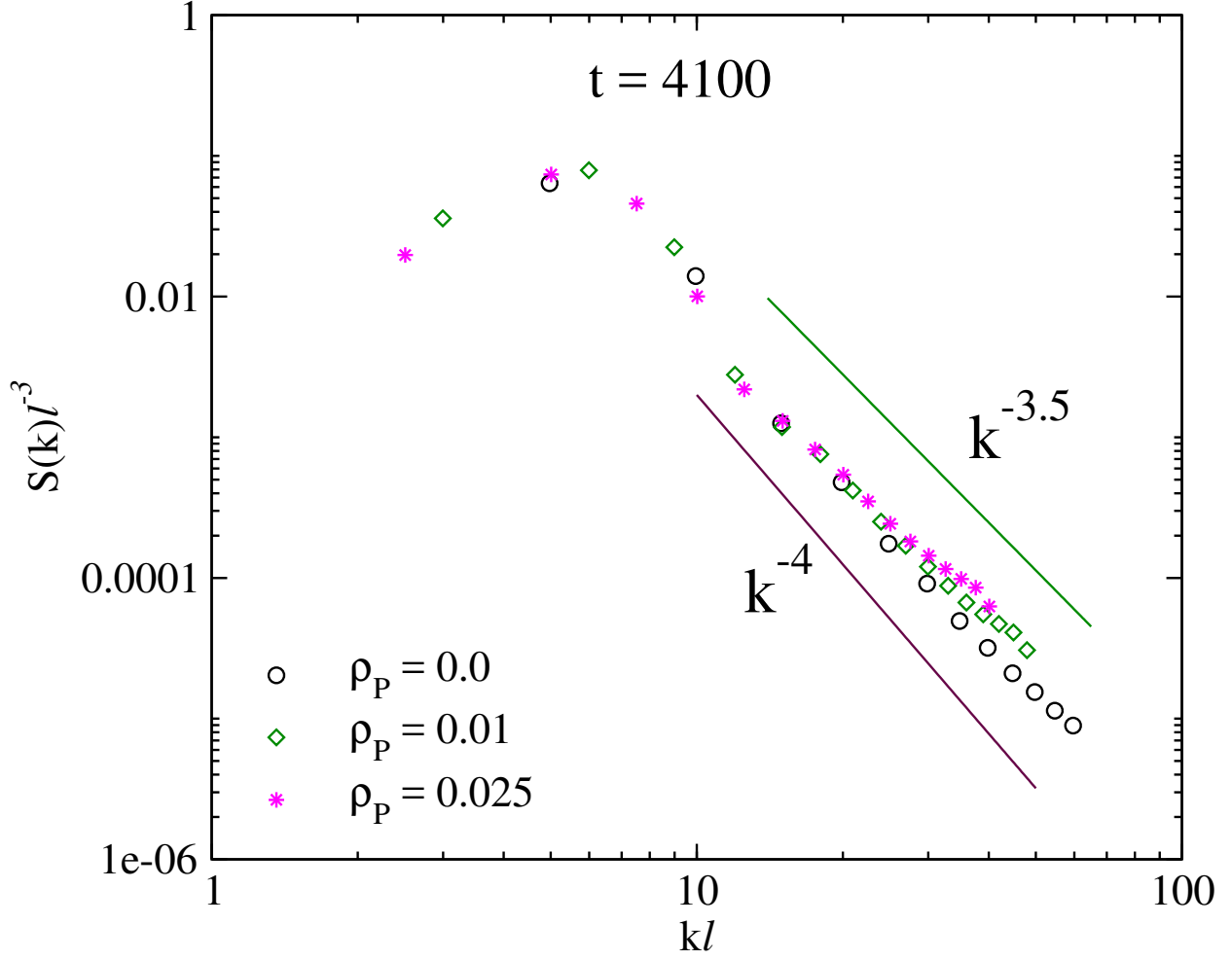


FIG. 5: The scaled structure factor $S(k)l^{-3}$ vs ℓk is plot (points) for three different ρ_P in the log-log scale. The straight lines are the guideline for the Porod law $S(k) \sim k^{-d+1}$ and the non-Porod behavior $S(k) \sim k^{-d+\delta}$ where $\delta = 0.5$ (see text).

Govt. of India (no. SRG/2019/001923) for financial support.

-
- [1] M.E. Fisher, Rep. Prog. Phys. **30**, 615–730 (1967).
 - [2] H.E. Stanley, Introduction to Phase Transitions and Critical Phenomena (Oxford University Press, 1971).
 - [3] K. Binder, Rep. Prog. Phys. **50**, 783–859 (1987).
 - [4] R.A.L. Jones, Soft Condensed Matter (Oxford University Press, 2002).
 - [5] A.J. Bray, Adv. Phys. **51**, 481–587 (2002).

- [6] K. Binder, Phys. Rev. B **15**, 4425–4447 (1977).
- [7] E. D. Siggia, Phys. Rev. A **20**, 595 (1979).
- [8] H. Furukawa, Phys. Rev. A **31**, 1103–1108 (1985).
- [9] M. San Miguel, Phys. Rev. A **31**, 1001–1005 (1985).
- [10] H. Tanaka, J. Chem. Phys. **103**, 2361 (1995).
- [11] D. Beysens, Y. Garrabos, D. Chatain, Europhys. Lett. **86**, 16003 (2009).
- [12] S. Tanaka, Y. Kubo, Y. Yokoyama, A. Toda, K. Taguchi, H. Kajioka, J. Chem. Phys. **135**, 234503 (2011).
- [13] V.M. Kendon, M.E. Cates, I. Pagonabarraga, J.C. Desplat, P. Blandon, J. Fluid Mech. **440**, 147–203 (2001).
- [14] S. Puri, B. Dünweg, Phys. Rev. A **45**, R6977–R6980 (1992).
- [15] C. Datt, S.P. Thampi, R. Govindarajan, Phys. Rev. E **91**, 010101(R) (2015).
- [16] M. Laradji, S. Toxvaerd, O.G. Mountain, Phys. Rev. Lett. **77**, 2253–2256 (1996).
- [17] A.K. Thakre, W.K. den Ohe, W.J. Briels, Phys. Rev. E **77**, 011503 (2008).
- [18] S. Ahmad, S.K. Das, S. Puri, Phys. Rev. E **82**, 040107 (2010).
- [19] K. Binder and D. Stauffer, Phys. Rev. Lett. **33**, 1006 (1974); Z. Phys. B **24**, 407 (1976).
- [20] K. Binder, in Phase Transformation of Materials, edited by R. W. Cahn, P. Haasen, and E. J. Kramer, Material Science and Technology (VCH, Weinheim, 1991), Vol. 5, p. 405; Kinetics of Phase Transitions, edited by S. Puri and V. Wadhawan (CRC Press, Boca Raton, 2009).
- [21] S. Puri, Phase Transitions **77**, 469 (2004).
- [22] D. A. Huse and C. L. Henley, Phys. Rev. Lett. **54**, 2708 (1985).
- [23] G. S. Grest and D. J. Srolovitz, Phys. Rev. B **32**, 3014 (1985).
- [24] D. J. Srolovitz and G. S. Grest, *ibid.* **32**, 3021 (1985).
- [25] S. Puri, D. Chowdhury and N. Parekh, J. Phys. A **24**, L1087 (1991).
- [26] A. J. Bray and K. Humayun, J. Phys. A **24**, L1185 (1991).
- [27] M. Rao and A. Chakrabarti, Phys. Rev. Lett. **71**, 3501 (1993).
- [28] R. Paul, S. Puri and H. Rieger, Europhys. Lett. **68**, 881 (2004); Phys. Rev. E **71**, 061109 (2005).
- [29] M. Henkel and M. Pleimling, Europhys. Lett. **76**, 561 (2006); Phys. Rev. B **78**, 224419 (2008).
- [30] C. Aron, C. Chamon, L. F. Cugliandolo and M. Picco, J. Stat. Mech., P05016 (2008); L. F. Cugliandolo, Physica A **389**, 4360 (2010).
- [31] F. Brochard and P. G. de Gennes, J. Phys. Lett. (Paris) **44**, 785 (1983).

- [32] P. G. de Gennes, *J. Phys. Chem.* **88**, 6469 (1984).
- [33] J. V. Maher, W. I. Goldberg, D. W. Pohl and M. Lanz, *Phys. Rev. Lett.* **53**, 60 (1984).
- [34] M. C. Goh, W. I. Goldberg and C. M. Knobler, *Phys. Rev. Lett.* **58**, 1008 (1987).
- [35] P. Wiltzius, S. B. Dierker and B. S. Dennis, *Phys. Rev. Lett.* **62**, 804 (1989).
- [36] S. K. Das, M. E. Fisher, J. V. Sengers, J. Horbach and K. Binder, *Phys. Rev. Lett.* **97**, 025702 (2006).
- [37] L. Verlet, *Phys. Rev.* **98**, 159 (1967).
- [38] D. Frenkel and B. Smit, *Understanding Molecular Simulations: From Algorithms to Applications* (Academic Press, San Diego, 2002).
- [39] G. P. Shrivastav, S. Krishnamoorthy, V. Banerjee and S. Puri, *Europhys Lett.* **96**, 36003 (2011).
- [40] Shaista Ahmad, Sanjay Puri and Subir K. Das, *Phys. Rev. E* **90**, 040302(R) (2014).
- [41] Z. W. Lai, G. F. Mazenko and O. T. Valls, *Phys. Rev. B* **37**, 9481 (1988).
- [42] F. Corberi, E. Lippiello, A. Mukherjee, S. Puri and M. Zannetti, *Phys. Rev. E* **85**, 021141 (2012).